

# Elastic properties of apatites

R. S. GILMORE\*, J. L. KATZ

*Center for Biomedical Engineering, Rensselaer Polytechnic Institute, Troy  
NY 12181, USA*

One of the prime motives for studying the elastic properties of the apatites stems from the occurrence of hydroxyapatite, OHAp, in calcified tissue. In this paper the isotropic elastic contents of crystalline apatite solids are determined from measurements of elastic wave velocities through powders under pressure. Once obtained, these elastic constants are used to model the elastic behaviour of a two-phase composite material having one phase more rigid than the other by a factor of 2.4. The results are then used in a general discussion of the probable order of magnitude of the elastic constants of the organic non-crystalline phase in bones and teeth, under the assumption of a two-phase system.

## 1. Introduction

### 1.1. Historical review

Reviews of the stress-strain behaviour in bone [1-3] and teeth [4] are available. Much of the work has been devoted to studying the effect of various factors such as microanatomy, inorganic content and age, on elastic properties. Most of the experiments have used standard mechanical testing procedures. However, a number of investigators have utilized ultrasonic techniques to study the elastic properties of hard tissue; Lees [5] summarizes and discusses these ultrasonic results.

Currey [6], and Bonfield and Li [7], respectively, in early papers summarized the state of knowledge concerning the elastic and inelastic properties of hard tissue. They both used an equivalent strain calculation, such as was first proposed by Voigt [8], in their discussion.

The present work shows why the equivalent strain model can be used only to indicate a lower or upper bound of the quantity being calculated depending, respectively, on whether the elastic moduli of one of the component phases is being calculated or those of the entire composite.

### 1.2. Introduction to experiment

High pressure ultrasonic studies of ClAp, FAp and OHAp give precise information on their elastic constants and equations of state. Ultrasonic

studies on single crystals compressed by hydrostatic pressure provide the most reliable and the greatest volume of information about the elastic properties of a crystal. These measurements for hexagonal and monoclinic crystals, however, require several relatively pure crystals, at least 1 cm on a side, cut to several orientations. Of the three apatites, only FAp is readily available in large single crystals, and since a comparative study of the three is desired, single-crystal studies are abandoned for the present.

The use of quasi-isotropic polycrystalline ceramics to study both the elastic constants of materials and their pressure and temperature derivatives has received much recent attention [9-11]. However, ClAp has been the only material of the three that has shown any tendency to sinter into a non-porous solid material. OHAp may decompose before suitable sintering temperatures are reached and FAp yields only a coarse and porous mass even for temperatures in the vicinity of 1000°C. Thus, studies of ceramics were also temporarily abandoned because of fabrication problems.

A third procedure was available. Several years of work in the geology department at Rensselaer Polytechnic Institute have been directed to the construction and calibration of a uniaxial high-pressure ultrasonic apparatus, Figs 1 and 2, with

\*Permanent address: Research and Development Center, General Electric Co., Building 37, Schenectady, New York 12345, USA.

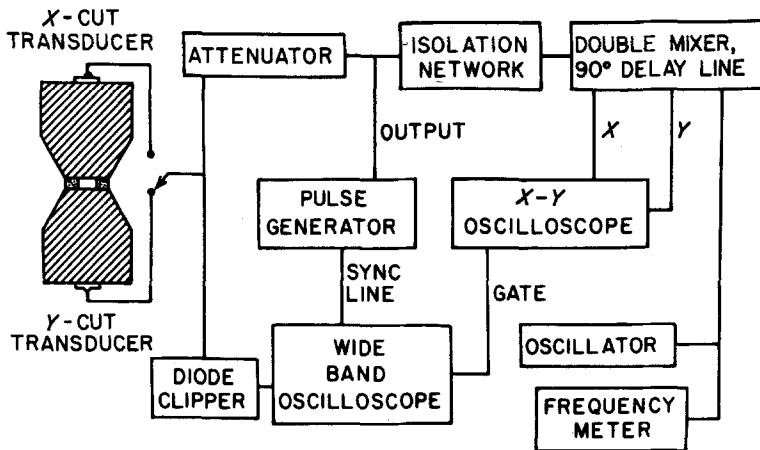


Figure 1 Schematic diagram of high pressure ultrasonic apparatus.

a pressure capability of  $10^{10} \text{ N m}^{-2}$  [12, 13]. Procedures have also been developed to make measurements on powdered materials. There are many minerals abundant in the earth's crust having sufficiently low symmetry that single-crystal measurements would be very tedious and for which sintering techniques are not yet developed. The following is a description of the results of measurements on powdered specimens of ClAp, FAp and OHAp to  $5 \times 10^9 \text{ N m}^{-2}$  in that apparatus.

## 2. Theory of measurement

### 2.1. Description

The apparatus and the calculation scheme used here are described elsewhere [13]. Briefly, the

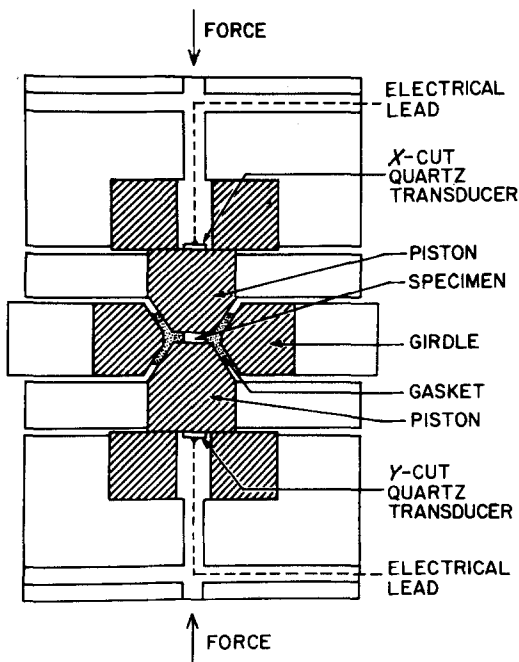


Figure 2 High pressure cell.

measurement consists of pelleting the powdered specimen in a small cylindrical die and then placing it in the high pressure apparatus for the ultrasonic velocity measurements.

Following interference techniques first developed by McSkimin [14], a radio frequency (r.f.) pulse is applied to either of the ultrasonic transducers mounted in the centre of the back face of the tungsten carbide pistons, see Figs 1 and 2. The resulting ultrasonic pulse is internally reflected within the pistons and specimen. Each transducer acts as both transmitter and receiver. When the ultrasonic pulse duration is greater than twice the transit time for the wave to pass through the specimen, interference occurs between the reflections from the near and far piston-specimen interfaces. In this condition the carrier frequency may be adjusted until successive reflections from the far piston-specimen boundary are all  $\pi$  radians out of phase with those from the near boundary. The conditions governing the resulting interference of the elastic waves permit the ultrasonic velocities to be calculated when the specimen thickness and the carrier frequency of the r.f. pulses are known.

### 2.2. Interferometry

For two waves of the same frequency, destructive interference occurs when they are  $\pi$  radians out of phase. Thus, for a specimen of thickness  $l$ , the condition for destructive interference as evident from the phase relationship between the reflections from the two anvil specimen interfaces is

$$2l + \frac{\theta\lambda}{2\pi} = \frac{\lambda}{2}(2n + 1); \quad n = 1, 2, 3, \dots, \quad (1)$$

where  $\lambda$  is the wavelength and  $\theta$  the total phase

shift in radians at the interfaces. Thus, minima in reflected energy occur where

$$l = \frac{\lambda}{2}, \frac{3\lambda}{2}, \frac{5\lambda}{2}, \dots, \text{etc.}$$

The velocity may now be written as

$$V = F\lambda = F_0(2l), F_1(\frac{4}{3}l), F_2(\frac{2}{3}l) \dots, \quad (2)$$

where  $F_{n+1} - F_n = F_0$ . Thus, measurements of the carrier frequency of the r.f. pulse at a minimum in reflected energy, and of the specimen thickness give the velocity directly.

### 2.3. Pressure—velocity relationship

Several procedures have been developed to evaluate the change in specimen thickness as a function of pressure. The first, and most straightforward, simply uses linear variable differential transformers (LVDT) to measure the piston displacement as pressure is increased. The piston deformation is then subtracted to arrive at the change in thickness of the specimen. A second procedure calculates the specimen deformation from the ultrasonic measurements by a numerical iteration using a high speed computer. Both procedures give the same results within experimental precision ( $\pm 5\%$ ).

The pressure corresponding to a given applied force on the tungsten carbide pistons is determined by observing changes in electrical resistance accompanying volume transitions in Bi and Ti that occur at known pressures. Pressures between these calibration points are obtained by interpolation. With the application of pressure, the elastic properties, thickness, and density of the specimen all change. Thus, in order to determine the elastic constants, the change in specimen density, thickness, and elastic velocity must be taken into account simultaneously.

For a homogeneous isotropic medium, the two solutions to the elastic wave equations correspond to longitudinal and transverse waves [15] propagating with velocities of

$$C_l = \left( \frac{K_s + \frac{4}{3} G_s}{\rho} \right)^{\frac{1}{2}} \quad (3)$$

and

$$C_\tau = \left( \frac{G_s}{\rho} \right)^{\frac{1}{2}}, \quad (4)$$

respectively, where  $K_s$ ,  $G_s$  and  $\rho$  are the adiabatic bulk modulus, adiabatic shear modulus and density, respectively. Thus, the elastic constants may

be written as

$$K_s = (C_l^2 - \frac{4}{3} C_\tau^2) \quad (5)$$

and

$$G_s = \rho C_\tau^2. \quad (6)$$

If the bulk modulus, measured during the adiabatic passage of an elastic wave, is used to calculate the change in specimen density due to an isothermal change in pressure, the standard thermodynamic correction must be applied. Here,

$$K_\tau = K_s / (1 + \alpha^2 T K_s / \rho C_p) = \rho \left. \frac{dP}{d\rho} \right|_\tau, \quad (7)$$

where  $K_\tau$ ,  $\alpha$ ,  $T$ ,  $\rho$  and  $C_p$  are the isothermal bulk modulus, thermal expansion, temperature, density, and specific heat at constant pressure, respectively. The combination of Equations 5 and 7 gives

$$d\rho = \left( 1 + \frac{\alpha^2 T K_s}{\rho C_p} \right) \left( \frac{\rho dP}{C_l^2 - \frac{4}{3} C_\tau^2} \right). \quad (8)$$

Thus, where the velocities are known a small change in density may be calculated from a small change in pressure. The summation of a large number of small changes is required to correctly calculate the density due to a large increase in pressure. Although for most materials, including the apatites, the adiabatic—adiabatic correction is only a few per cent, it involves both  $\alpha$  and  $C_p$ , so a brief discussion of their pressure dependence is in order. An assumption often used in high pressure research is that  $\gamma C_v / V$  is independent of pressure [16], where  $\gamma$ ,  $C_v$ , and  $V$  are the Gruneisen ratio, specific heat at constant volume, and specific volume, respectively. Thus, with  $K_\tau \alpha = \gamma C_v / V$  [17], the pressure dependence of  $\alpha$  may be shown to vary as the inverse of the pressure dependence of the isothermal bulk modulus. Additional calculations [13] show that  $C_p$  varies only 10% in  $10^{11} \text{ N m}^{-2}$  and thus may be taken to be nearly independent of pressure.

### 2.4. Effects of porosity

The use of compacted powder as the specimen introduces the difficulty of porosity at lower pressures. The initial dramatic increase in the elastic velocities shown in Fig. 3 is primarily due to compression of the pores. Velocity—pressure curves in non-porous solids show little or no curvature [9, 11, 18], while studies in rocks and similar porous structures show considerable curvature at low pressure [16]. In this work, the

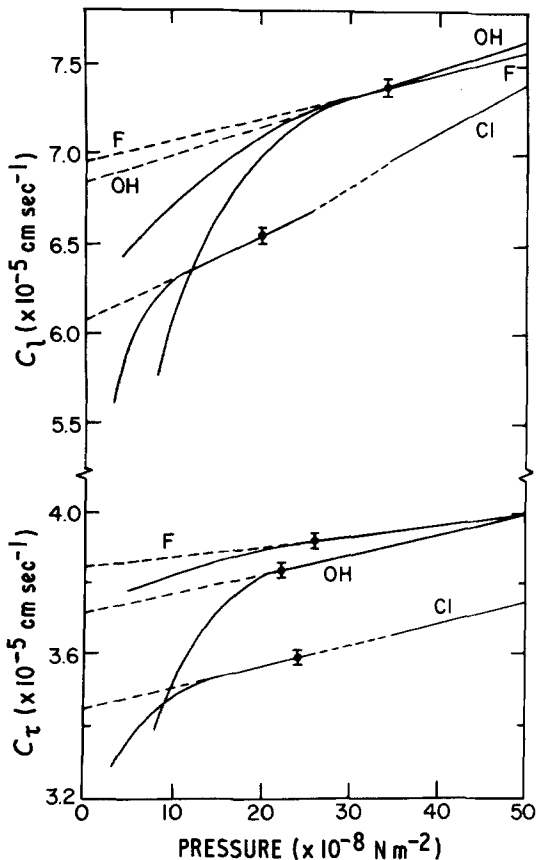


Figure 3 Longitudinal and transverse velocities in OHAp, FAp, and ClAp to  $5 \times 10^9 \text{ N m}^{-2}$ .

pressure where the porosity becomes zero has been interpreted as the pressure at which the velocity–pressure relationship becomes linear. The porosity returns as pressure is released, however, because the temperature (298 K) is too low for self-diffusion and sintering to occur. The velocity values that would occur in a sintered polycrystalline solid of ClAp, FAp, and OHAp near zero pressure are predicted by extrapolating the linear high pressure relationship back to zero pressure.

Several reviews [19–21] show that both the elastic velocities and moduli of all non-porous materials measured to date may be approximated closely by linear functions in pressure. Present exceptions to this occur only in the case of first order polymorphic transitions during which there are discontinuous changes in the density, velocity, and moduli relationships, when pressure is the independent variable. By use of the above information, elastic-moduli–pressure relationships may be developed by extrapolating the linear portion back to zero pressure to give

$$M = M_0 + M'P, \quad (9)$$

where  $M$ ,  $M_0$ ,  $M'$  and  $P$  are the elastic modulus, its value at zero pressure, its pressure derivative and the pressure at which it is evaluated, respectively.

The specimen density after the pores are closed is calculated from the zero pressure crystalline density and the extrapolated velocity values, Fig. 3, using Equation 8. In this work the elastic behaviour of the powder at pressures where it is porous has been neglected. If this information is desired, the zero-pressure density of the porous pellet must be determined by mercury displacement techniques. Once this is known, the change in density of porous mediums may be calculated from the measured velocities, again with Equation 8.

### 2.5. OHAp–NaCl composite

Since hard tissue is a composite, a natural extension of this work is the measurement of the behaviour of OHAp in a two-phase composite. Sodium chloride was chosen as the second member because of its ability to sinter at room temperature and its low elastic moduli compared with OHAp. The latter feature is important because the non-crystalline phases in hard tissue have considerably lower elastic moduli than does crystalline apatite.

The elastic properties of a composite, composed of two materials whose elastic moduli are known, is considered in the most general way by Hill [22]. Simmons and Chung [23] have applied Hill's work to determine the elastic constants of an unknown crystalline material by imbedding it in a matrix with known elastic properties and then determining the unknown by measuring the elastic properties of the composite.

The application of a rigorous elasticity calculation based on a two-phase composite, while applicable to the apatite–NaCl mixtures, is not necessarily applicable to hard tissue. Current theories regarding the existence of crystalline, amorphous and organic components and their fractional concentrations should receive primary attention in the development of a model for the elastic behaviour for bone and teeth. In addition, the elastic moduli of materials with low shear strengths, such as long-chain organic molecular solids, increase with increasing strain rate. The values for elastic moduli calculated from wave velocities are at maximum strain rates and hence are maximum values. These may be quite different

from those obtained in standard compression and tension tests or from those determined when the elastic response of a skeleton is stressed by the actions of a living organism.

An approximate treatment that assumes strain throughout the mixture is uniform [8] gives

$$K_v = C_1 K_1 + C_2 K_2 \quad (10)$$

and

$$G_v = C_1 G_1 + C_2 G_2, \quad (11)$$

where  $K_v$ ,  $K_1$ ,  $K_2$ ,  $G_v$ ,  $G_1$ ,  $G_2$ ,  $C_1$  and  $C_2$  are the bulk moduli of the composite and two phases, the shear moduli of the composite and two phases and the fractional volume concentrations of the two phases, respectively. The dual assumption, due to Reuss [24], is that stress is uniform. This gives

$$\frac{1}{K_R} = \frac{C_1}{K_1} + \frac{C_2}{K_2} \quad (12)$$

and

$$\frac{1}{G_R} = \frac{C_1}{G_1} + \frac{C_2}{G_2}, \quad (13)$$

where  $K_R$  and  $G_R$  are the bulk and shear moduli of the composite, respectively. Hill [22] has shown by elementary considerations of the strain energy that the actual bulk modulus of the composite falls between the Voigt and the Reuss approximations as upper and lower bounds. However, these bounds become quite large, see Fig. 4, when the elastic modulus of one phase differs from the other by a factor greater than 2.

The solutions of Equations 10 to 13 in terms of one of the phases now give a method for placing upper and lower bounds on the other phase. Thus, Equations 10 to 13 give

$$K_1 = \frac{K_v - C_2 K_2}{C_1}, \quad (14)$$

$$G_1 = \frac{G_v - C_2 G_2}{C_1}, \quad (15)$$

$$K_1 = \frac{C_1 K_R K_2}{K_2 - C_2 K_R} \quad (16)$$

and

$$G_1 = \frac{C_1 G_2 G_R}{G_2 - C_2 G_R}, \quad (17)$$

respectively. It will be noted that, in the use of the measured composite moduli with the known

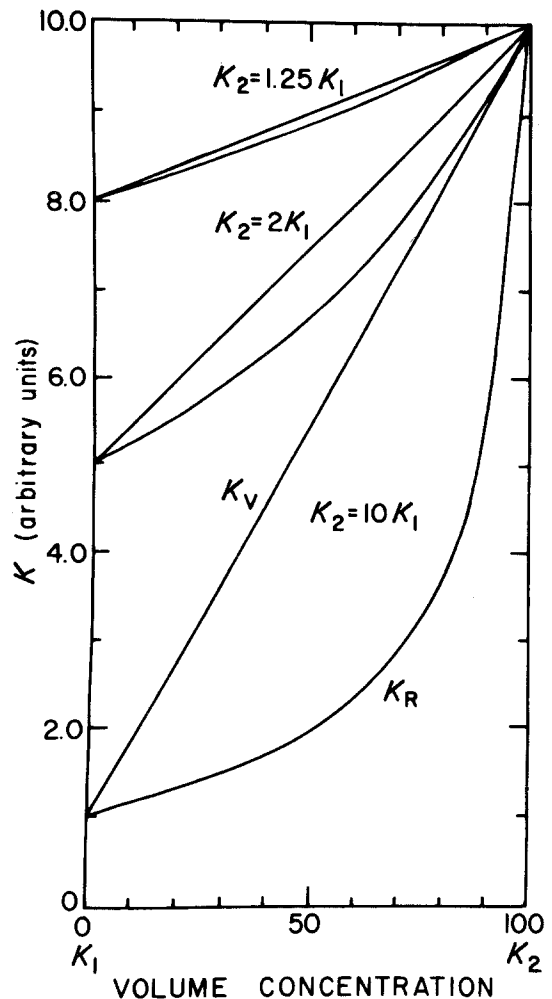


Figure 4 Voigt-Reuss limits for the bulk modulus of two-phase composites where  $8K_2 = 10K_1$ ,  $K_2 = 2K_1$  and  $K_2 = 10K_1$ .

moduli of one phase to calculate values for the other, the Voigt equations give a lower bound value and the Reuss equations an upper bound.

The elastic moduli of OHAp and the bulk measurements of hard tissue (dentin and enamel) now permit us to place bounds on the elastic properties of the material present other than crystalline apatite. It should be emphasized, however, that the calculations outlined above implicitly assume the apatite is randomly oriented and that only one other phase is present. Thus, the organic and possible amorphous phase are treated as one. It should also be emphasized that the large contrast in the moduli of the crystalline and non-crystalline phases in hard tissue make calculations very imprecise.

TABLE I Pressure dependence of sonic velocities

Material	Density, $\rho$ (g cm <sup>-3</sup> )	Longitudinal velocity, $C_l$ (km sec <sup>-1</sup> )	Transverse velocity, $C_t$ (km sec <sup>-1</sup> )
OHAp	3.17	$6.85 + 0.16 P^*$	$3.75 + 0.056 P$
FAP	3.18	$6.95 + 0.12 P$	$3.82 + 0.030 P$
ClAp	3.12	$6.10 + 0.23 P$	$3.45 + 0.060 P$
Dentin [25]	2.2	3.6	1.9
Enamel [25]	2.9	5.4	3.2
NaCl	2.16	$4.62 + 0.18 P$	$2.58 + 0.070 P$

\* $P$  is in GN m<sup>-2</sup>. Overall precision is  $\pm 2\%$ .

### 3. Experimental procedure

The experimental procedure consists of pelleting each specimen into a right circular cylinder 0.350 cm thick and 0.635 cm in diameter, cycling it twice to a pressure of  $5 \times 10^9$  N m<sup>-2</sup> and taking ultrasonic data on the third cycle. The data, taken at 2 and  $5 \times 10^8$  N m<sup>-2</sup> intervals for both increasing and decreasing pressure, consist of measurements of the force applied to the high pressure cell, Fig. 1, by a hydraulic press, of several frequencies at successive minima, and of the piston displacement.

The high pressure cycling serves the dual purpose of compacting the specimen and providing a reproducible pressure. The known polymorphic transitions used to provide the force-pressure calibration usually do not occur at reproducible values of applied force until after the second or third cycle.

### 4. Results

Ultrasonic data were taken on three specimens of FAp, OHAp, and ClAp, respectively. Both the FAp and OHAp specimens were pelleted from natural minerals not less than 90% pure. The ClAp specimens were pelleted from synthetic materials, prepared in the Materials Engineering Department at Rensselaer Polytechnic Institute. The natural apatite samples used in these measurements were selected so that impurities were small. The minerals that typically occur in natural apatite have elastic properties closely approximating those of the host material. Estimates made using composite calculations described by Equations 10 to 13 indicate that errors due to impurities affect the elastic constants measured here by less than 2%.

However, one effect that could be significant is the tendency of impurities to suppress polymorphic transitions in their host. The fact that a velocity discontinuity was found in the pure ClAp but not in the natural materials, could

be due either to a lack of discontinuities in these materials or to their suppression by the impurities.

The ultrasonic velocities for FAp, OHAp, and ClAp are shown in Fig. 3 and Table I. The relationships shown in Table I result from expressing the linear portion of the velocity data as a straight-line equation. Extrapolation of this straight line back to atmospheric pressure gives the approximate velocity in a sintered solid with no porosity.

The elastic constants shown in Figs 5, 6 and 7 and Table II are calculated directly from the velocity data.

The velocity discontinuity in the ClAp data suggests that a polymorphic transition occurs in

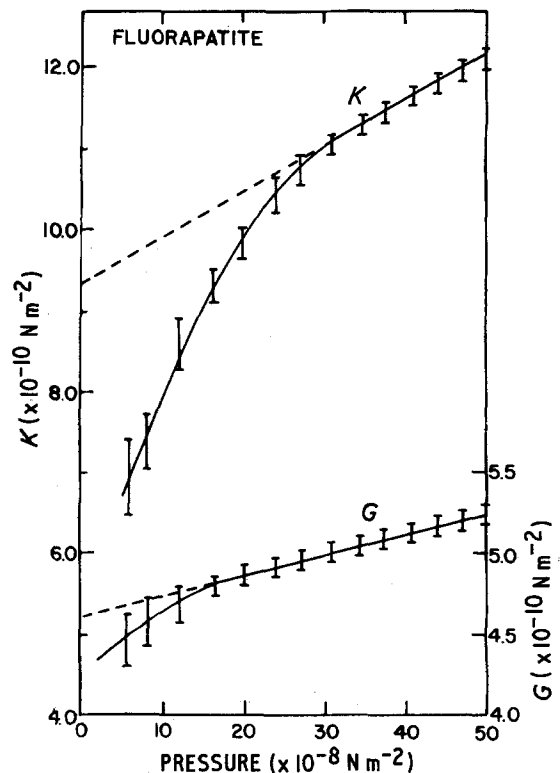


Figure 5 The elastic constants of OHAp to  $5 \times 10^9$  N m<sup>-2</sup>.

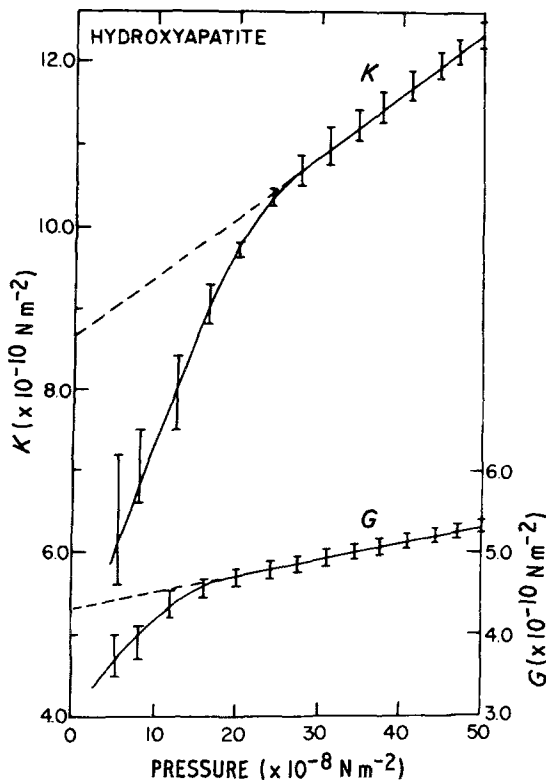


Figure 6 The elastic constants of FAP to  $5 \times 10^9 \text{ N m}^{-2}$ .

ClAp between  $26$  and  $30 \times 10^8 \text{ N m}^{-2}$ . Although a change in slope has been found in the pressure–volume curve, the volume measurements do not have sufficient precision to determine the magnitude of volume change associated with the phase transition. Speculation based on the amount of force required to drive the volume change to completion indicates that the volume changes a few per cent.

The elastic behaviour of the 50–50 and 20–80 NaCl–OHAp composites is summarized in Figs 8 to 11. Fig. 12 shows that the bulk values follow the Reuss approximation more closely than they do the Voigt approximation.

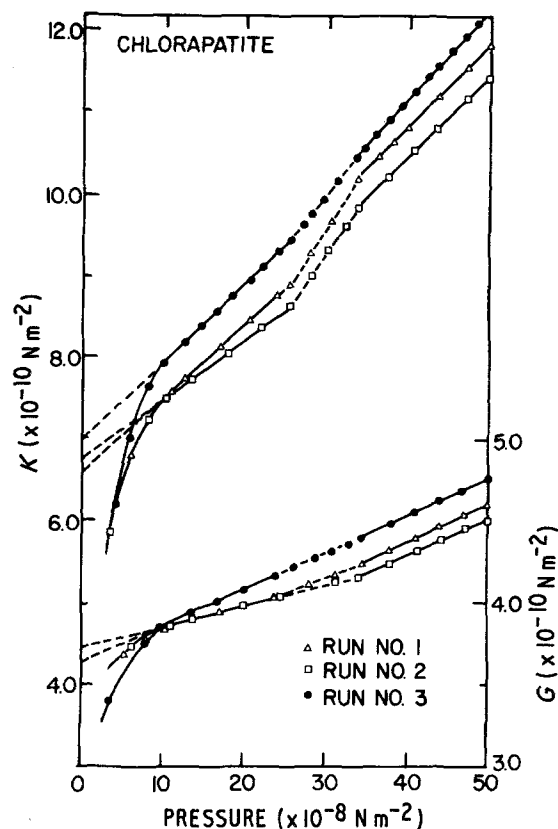


Figure 7 The elastic constants of ClAp to  $5 \times 10^9 \text{ N m}^{-2}$ .

Ultrasonic velocities performed on slices of bovine dentin and enamel [24] may now be used to give an indication of the sonic moduli of collagen, see Fig. 13. The Reuss approximation is used in the calculation because the non-linearity of the elastic moduli, as a function of the volume concentration of OHAp, suggests this would give the most nearly precise results. The resultant values for the bulk and shear moduli are  $0.82 \times 10^{10} \text{ N m}^{-2}$  and  $0.55 \times 10^{10} \text{ N m}^{-2}$ , respectively. It should be remembered that these are for the combination of the amorphous and organic phases as one phase and that their physical significance is that of an upper bound.

TABLE II Zero pressure values and pressure derivatives of the ultrasonic moduli of elasticity\*

Material	$K_s$ ( $\times 10^{10} \text{ N m}^{-2}$ )	$K'_s$	$G_s$ ( $\times 10^{10} \text{ N m}^{-2}$ )	$G'_s$	$E_s$ ( $\times 10^{10} \text{ N m}^{-2}$ )
OHAp	8.90	6.9	4.45	1.6	11.4
FAP	9.40	5.8	4.64	1.3	12.0
ClAp (0 to $26 \times 10^8 \text{ N m}^{-2}$ )	6.85	8.5	3.71	2.2	9.43
Dentin [25]	1.8	—	0.80	—	2.1
Enamel [25]	4.6	—	3.0	—	7.4
NaCl	2.60	4.7	1.45	1.0	3.67

\*Overall accuracy is  $\pm 1\%$  for both the bulk modulus,  $K_s$ , and the shear modulus,  $G_s$ . The pressure derivatives,  $K'_s$  and  $G'_s$  are accurate to 8%.

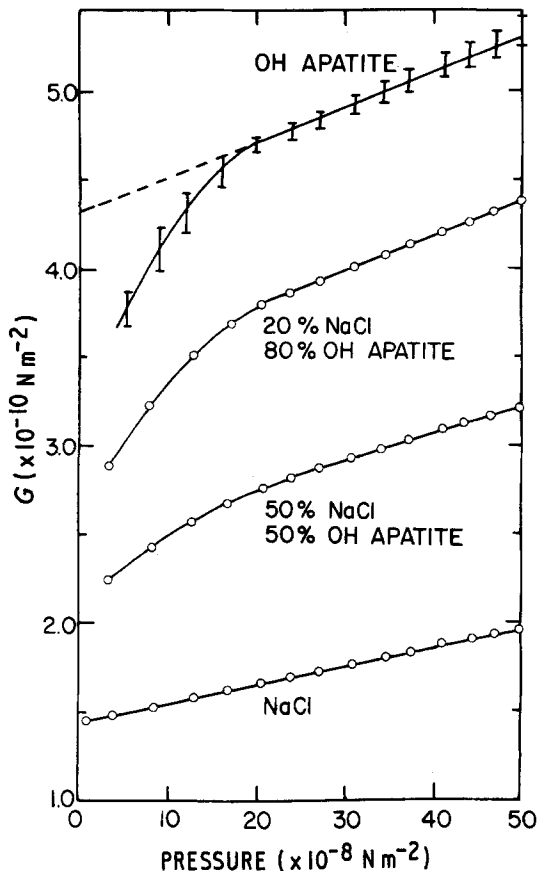


Figure 8 The pressure dependence of the shear modulus of NaCl-OHAp composites.

## 5. Discussion

The modulus most often measured on biological materials is Young's modulus. In the usual experiment, oriented sections of bone or teeth are loaded in tension or compression, and the axial force and resultant strain are measured. The dependence of the elastic moduli of composite materials, where the phases are markedly different, on strain rate and strain amplitude is too extensive to be discussed in detail here. It is sufficient to say that the elastic moduli increase with strain rate. Thus, since ultrasonic velocities are the maximum rates for the propagation of strain and stress through materials, they should give the maximum elastic moduli for those materials.

Variations of crystallinity and structure in specimens prepared from bone and teeth give further sources of scatter. Fig. 13, shows that a 5% increase in the crystallinity of enamel could result in a 20% increase in the bulk and shear moduli.

The volume concentrations of OHAp, 90%

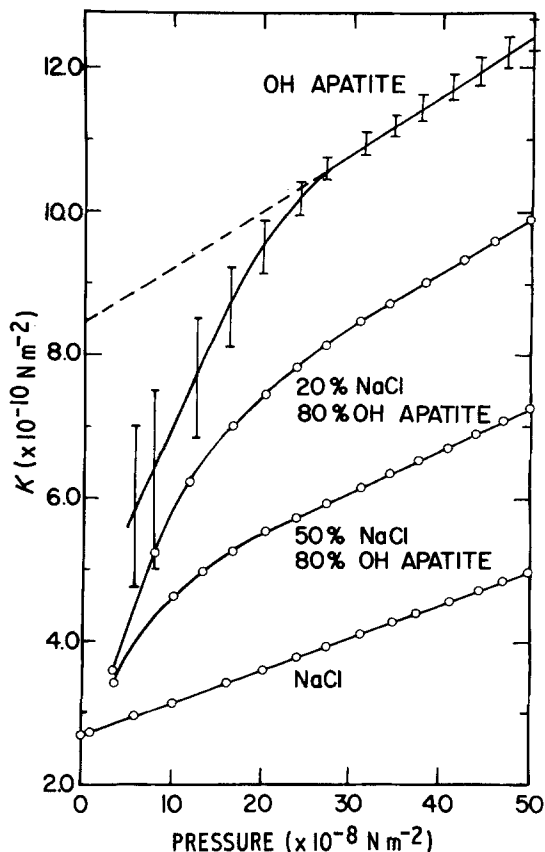


Figure 9 The pressure dependence of the bulk modulus of NaCl-OHAp composites.

and 60% for enamel and dentin, respectively, were chosen as generally representative, and it should not be inferred that they were measured. Investigators who prefer different representative values for bovine dentin and enamel based on their volume concentration measurements should feel free to reinterpret the ultrasonic data.

Fig. 13 also shows that attempts to fit the dentin, enamel and OHAp data to a straight line would result in negative values for the second phase. Thus, the linear (Voigt) approximation would appear to be less applicable than the Reuss calculation used here. Young's modulus may be calculated from the bulk and shear moduli. Thus, using  $K = 0.8 \times 10^{10} \text{ N m}^{-2}$  and  $G = 0.5 \times 10^{10} \text{ N m}^{-2}$ , one determines from

$$E = \frac{9KG}{3K + G}, \quad (18)$$

that the value for collagen from these calculations would be  $1.2 \times 10^{10} \text{ N m}^{-2}$ . Using this value for



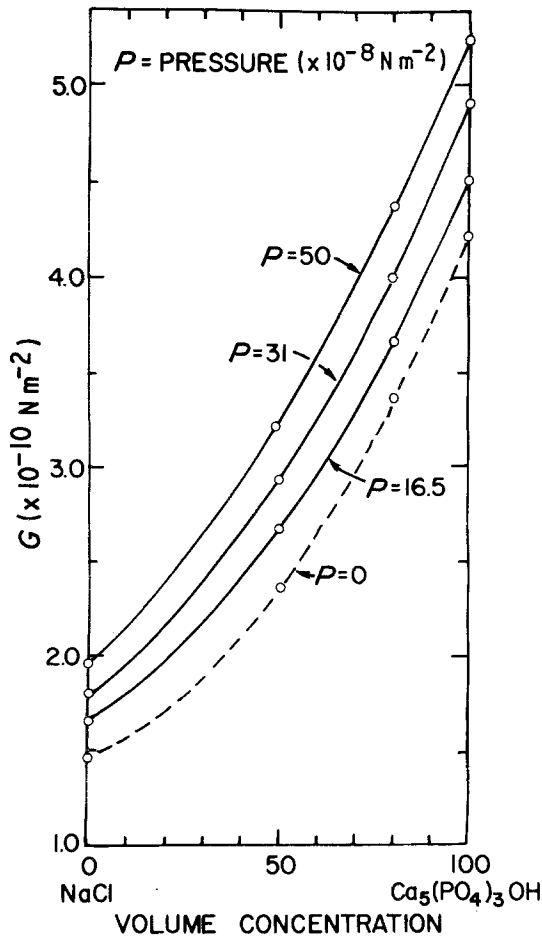


Figure 10 Dependence of the shear modulus of NaCl-OHAp composites on volume concentration.

collagen and  $11.4 \times 10^{10} \text{ N m}^{-2}$  for OHAp, Reuss' calculation gives 2 to  $3 \times 10^{10} \text{ N m}^{-2}$  for Young's modulus of a material 40% to 50% crystalline, or one close to bone in composition.

It should be emphasized that these calculations are based on sonic moduli and the Reuss approximations, and therefore represent an upper bound for collagen; values obtained with slower strain rates and/or with other approximations may fall well below these values. The Young's modulus for collagen calculated above is an order of magnitude greater than that reported by Currey [6],  $0.12 \times 10^{10} \text{ N m}^{-2}$ . However, the differences between ultrasonic and mechanical experiments make their comparison impossible without additional measurements at intermediate rates of strain.

Comparisons between this work and that of Yoon and Newnham [26] on FAp show the bulk and shear moduli measured here to be approxi-

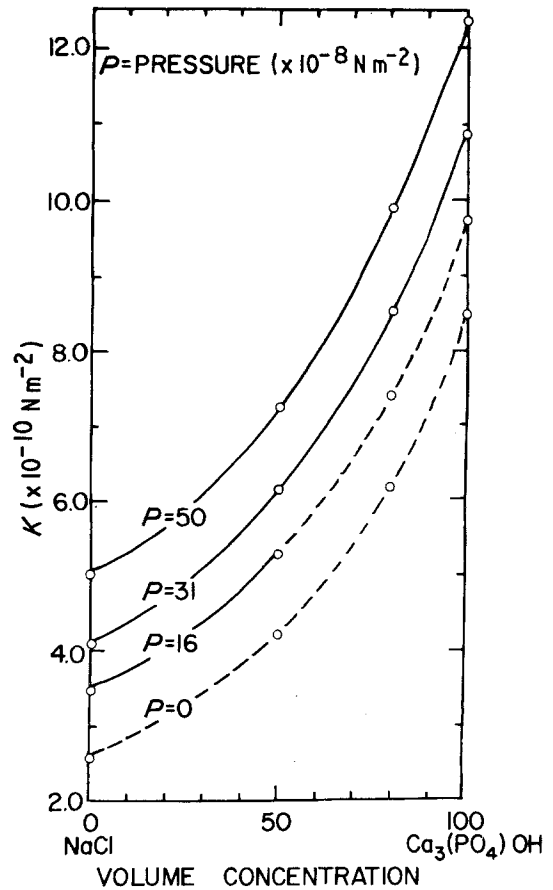


Figure 11 Dependence of the bulk modulus of NaCl-OHAp composites on volume concentration.

mately 10% larger than their values. This could be due to the preferred orientation of the particles in our samples due to uniaxial compression. Since all three apatites are similar in crystal structure, roughly identical compression textures should be formed in each so comparisons between the materials are unaffected by preferred orientation.

## 6. Summary

The study of stress and strain in bones and teeth has been of major interest to many investigators for the past 120 years. Today there is an extensive bibliography of elastic moduli studies on hard tissue. The largest portion of the work has been done using tension and compression machines at reasonably slow strain rates. However, there has been little written that recognizes the effect of strain rate and sample size on the resulting elastic moduli. There also have been few attempts to evaluate the elastic behaviour of the separate

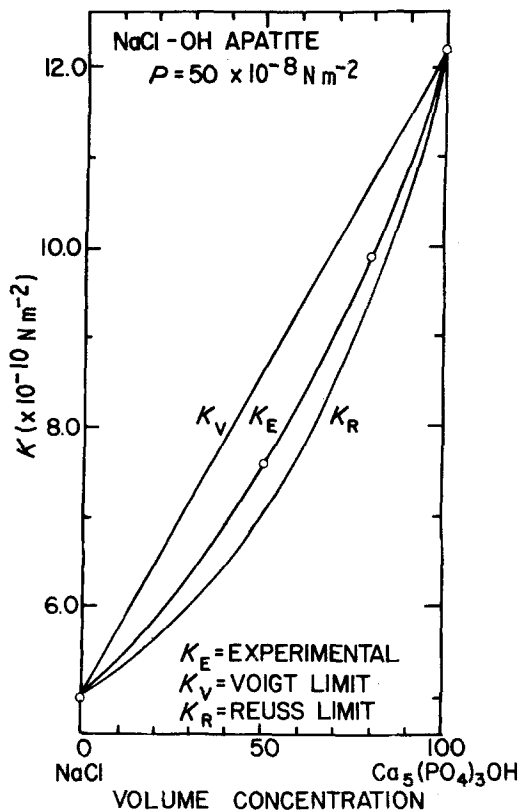


Figure 12 A comparison between the dependence of the bulk modulus of NaCl-OHAp.

components of hard tissue in order to develop a model to predict their composite properties.

This work described a series of measurements to evaluate the polycrystalline, quasi-isotropic elastic properties of OHAp, ClAp, and FAp. The data were taken by compacting powders to very high pressures ( $5 \times 10^9 \text{ N m}^{-2}$ ) and observing the velocity-pressure relationships after porosity had been removed. The velocities at zero pressure were then evaluated by backward extrapolation of the high pressure data.

Since hard tissue is composed of physically intermingled compounds, an attempt has been made to show how the compositional variations in mixtures of NaCl and OHAp affect elastic properties. NaCl was chosen as the other component because of its ability to sinter into a solid under high pressure at room temperature, its low elastic moduli compared with OHAp, and finally, because it is a well known material and can serve as a standard.

Velocity measurements on natural materials prepared from slices of dentin, enamel and com-

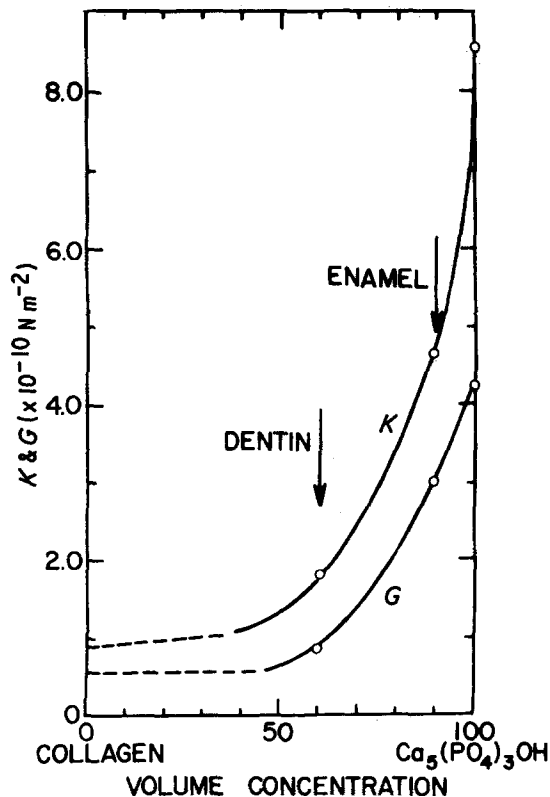


Figure 13 The elastic constants of hard oral tissue as a function of crystalline content. The extrapolation to evaluate the non-crystalline phase is based on the Reuss equation.

packed pellets of deorganified bone give comparisons between these, the pure apatite powders, and the OHAp-NaCl composites.

In general, the compressional velocities at zero pressure in all of the natural and synthetic apatites measured fall between  $6.5$  and  $7.0 \text{ km sec}^{-1}$ , with ClAp being consistently lowest. The shear velocities fall between  $3.5$  and  $4.0 \text{ km sec}^{-1}$ , again with ClAp being the lowest. The shear velocities in bovine dentin and enamel are  $1.9$  and  $3.2 \text{ km sec}^{-1}$ , respectively; the compressional velocities are  $3.6$  and  $5.4 \text{ km sec}^{-1}$ . The velocities in compacted, deorganified bone powders prepared from various species of fish are in the neighbourhood of  $5.0$  and  $2.7 \text{ km sec}^{-1}$ , respectively, for the compressional and shear velocities [27].

Additional equation-of-state information such as the elastic constants, Debye temperature, and pressure-volume behaviour have been obtained directly from the high pressure ultrasonic measurements.

A number of additional measurements on thermal, mechanical and elastic properties of

apatites and hard tissues have been reported in the literature. These measurements have been summarized, critically analysed and used for comparison where pertinent.

### Acknowledgements

The co-operation of Dr Samuel Katz, of the Geology Department at Rensselaer Polytechnic Institute is deeply appreciated. Valuable assistance was provided by Karl L. Dunn, Robert H. Courtney, and Dale E. Grenoble in various phases of the experiments. This research was supported in part by Grants 5 PO1 DE 2336-02 and 5 TL DE 0117-05 from the National Institute of Dental Research of the USPHS, and by NASA through the Rensselaer Interdisciplinary Materials Research Center.

### References

1. J. L. KATZ, in "The Mechanical Properties of Biological Materials", edited by J. F. V. Vincent and J. D. Currey (Cambridge University Press, Cambridge, 1980) p. 137.
2. F. G. EVANS, "Mechanical Properties of Bone" (Charles C. Thomas, Springfield, IL., 1973).
3. A. R. LIBOFF and M. H. SHAMOS in "Biological Mineralization", edited by I. Zipkin (John Wiley, New York, NY, 1973) p. 335.
4. N. E. WATERS in "The Mechanical Properties of Biological Materials", edited by J. F. V. Vincent and J. D. Currey (Cambridge University Press, Cambridge, 1980) p. 99.
5. S. LEES, *Archs. Oral Biol.* **13** (1968) 1491.
6. J. D. CURREY, *Biorheology* **2** (1964) 1.
7. W. BONFIELD and C. H. LI, *J. Appl. Phys.* **38** (1967) 2450.
8. W. VOIGT, "Lehrbuch der Kristalphysik" (Springer-Verlag, Berlin, 1928).
9. O. L. ANDERSON and E. SCHREIBER, *J. Amer. Ceram. Soc.* **49** (1966) 184.
10. E. SCHREIBER and O. L. ANDERSON, *J. Geophys. Res.* **71** (1966) 3002.
11. N. SOGA, *ibid.* **73** (1968) 5385.
12. T. J. AHRENS and S. KATZ, *ibid.* **68** (1963) 529.
13. R. S. GILMORE, Ph. D. Thesis (Rensselaer Polytechnic Institute, Troy, NY, 1968).
14. H. J. McSKIMIN, *Proc. Nat. Elec. Conf.* **XII** (1956) 1228.
15. A. E. H. LOVE, "The Mathematical Theory of Elasticity" (Dover Press, New York, NY, 1944).
16. F. BIRCH, *J. Geophys. Res.* **65** (1967) 1083.
17. J. C. SLATER, "Introduction to Chemical Physics" (McGraw-Hill Book Co, New York, NY, 1939).
18. N. SOGA, *J. Geophys. Res.* **72** (1967) 5157.
19. O. L. ANDERSON, *J. Phys. Chem. Solids.* **27** (1966) 547.
20. O. L. ANDERSON and R. C. LIEBERMANN in "Physical Acoustics, Principles and Methods", Vol. VI, Part B, edited by W. P. Mason (Academic Press, New York, 1968) p. 329.
21. G. SIMMONS, *Proc. IEEE* **53** (1965) 1337.
22. R. HILL, *J. Mech. Phys. Solids* **11** (1963) 357.
23. G. SIMMONS and D. H. CHUNG, *Trans. Amer. Geophys. U.* **49** (1968) 308.
24. E. REUSS in "Elastic Constants of Crystals", edited by H. B. Huntington (Academic Press, New York, NY, 1958).
25. R. S. GILMORE, R. POLLACK and J. L. KATZ, *Archs. Oral Biol.* **15** (1970) 787.
26. H. S. YOON and R. E. NEWNHAM, *Amer. Miner.* **54** (1969) 1193.
27. D. E. GRENOBLE, J. L. KATZ, K. L. DUNN, R. S. GILMORE and K. LINGA MURTY, *J. Biomed. Mat. Res.* **6** (1972) 221.

Received 3 August  
and accepted 19 September 1981.